BJP BRITISH JOURNAL OF PHARMACOLOGY

BPS BRITISH PHARMACOLOGICAL SOCIETY

British Journal of Pharmacology (2010), 160, 1302–1315

0007-1188/10
www.brjpharmacol.org

RESEARCH PAPER

Block and allosteric modulation of GABAergic currents by oenanthotoxin in rat cultured hippocampal neurons

Paulina Wyrembek[1], Katarzyna Lebida[1], Katarzyna Mercik[1], Katarzyna Szczuraszek[1], Marcin Szczot[1], Federica Pollastro[2], Giovanni Appendino[2] and Jerzy W Mozrzymas[1]

[1]*Laboratory of Neuroscience, Department of Biophysics, Wrocław Medical University, ul. Chałubińskiego, Wrocław, Poland, and* [2]*Dipartimento di Scienze Chimiche, Alimentari, Farmaceutiche e Farmacologiche, Via Bovio, Novara, Italy*

Background and purpose: Oenanthotoxin (OETX), a polyacetylenic alcohol from plants of the genus *Oenanthe*, has recently been identified as potent inhibitor of GABA-evoked currents. However, the effects of OETX on the inhibitory postsynaptic currents (IPSCs), as well as the pharmacological mechanism(s) underlying its effects on $GABA_A$ receptors, remain unknown. The purpose of this study was to elucidate the mechanism underlying the inhibition of GABAergic currents by OETX.
Experimental approach: Effects of OETX on GABAergic currents were studied using the patch clamp technique on rat cultured hippocampal neurons. Miniature IPSCs (mIPSCs) were recorded in the whole-cell configuration, while the current responses were elicited by ultrafast GABA applications onto the excised patches.
Key results: OETX potently inhibited both mIPSCs and current responses, but its effect was much stronger on synaptic currents. Analysis of the effects of OETX on mIPSCs and evoked currents disclosed a complex mechanism: allosteric modulation of both $GABA_A$ receptor binding and gating properties and a non-competitive, probably open channel block mechanism. In particular, OETX reduced the binding rate and nearly abolished receptor desensitization. A combination of rapid clearance of synaptic GABA and OETX-induced slowing of binding kinetics is proposed to underlie the potent action of OETX on mIPSCs.
Conclusions and implications: OETX shows a complex blocking mechanism of $GABA_A$ receptors, and the impact of this toxin is more potent on mIPSCs than on currents evoked by exogenous GABA. Such effects on GABAergic currents are compatible with the convulsions and epileptic-like activity reported for OETX.
British Journal of Pharmacology (2010) **160,** 1302–1315; doi:10.1111/j.1476-5381.2010.00644.x

Keywords: oenanthotoxin; $GABA_A$ receptor; mIPSC; binding; gating

Abbreviations: CGP 55845, ((2*S*)-3-[[(1*S*)-1-(3,4-dichlorophenyl)ethyl]amino-2-hydroxypropyl] (phenylmethyl) phosphinic acid); mIPSC, miniature inhibitory postsynaptic current; OETX, oenanthotoxin; RT, rise time

Introduction

Oenanthotoxin (OETX) is a polyacetylenic alcohol (Figure 1) typically found in plants from the genus *Oenanthe* (Umbelliferae family; Clarks *et al.*, 1949; Anet *et al.*, 1953). Plants from this genus are among the most poisonous species of the European flora, and have been used for ritual killing in pre-Roman Sardinia and other areas of Punic influence (Teuscher and Lindequist, 1994; Bruneton, 1999). Interestingly, poisoning with these plants induces contraction of the facial muscles, resulting in an expression that resembles a sinister smile (*risus sardonicus*, sardonic smile). Descriptions of *Oenanthe* and/or OETX action on humans and animals are well documented in the modern toxicological literature (Downs *et al.*, 2002), but, surprisingly, relatively little is known of the molecular target(s) of OETX and the mechanism(s) underlying its toxic actions. Dubois and Schneider (1981; 1982) have reported that OETX induced convulsions in rat, and that it reversibly blocked action potentials, as well as Na^+ and K^+ gating currents. Louvel and Heinemann (1980) have also found that OETX induced long-lasting epileptic activity in the cat cortex, and suggested that this effect could be due to an increase in calcium conductance in cortical cells. It seems that the most prominent action of OETX on the CNS is induction of epileptic-like activity (see also Chauvel *et al.*, 1978; Louvel and Heinemann, 1980; 1983; Ball *et al.*, 1987). Taking into

Correspondence: Jerzy W Mozrzymas, Laboratory of Neuroscience, Department of Biophysics, Wrocław Medical University, ul. Chałubińskiego 3, 50-367 Wrocław, Poland. E-mail: mozrzy@biofiz.am.wroc.pl
Received 23 June 2009; revised 27 November 2009; accepted 14 December 2009

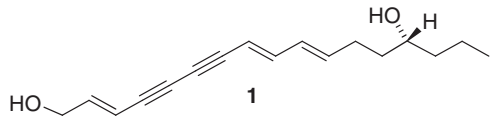

Figure 1 Structure of OETX.

account that one of the most common mechanisms of epilepsy is a dysfunction of neuronal inhibition, we have recently addressed the effect of OETX on ionotropic $GABA_A$ receptors (receptor nomenclature follows Alexander *et al.*, 2009) in cultures of rat neurons (Appendino *et al.*, 2009), and found that this toxin potently inhibits these channels. It is thus interesting to provide a more detailed description of pharmacological mechanism underlying the inhibitory effects of OETX on $GABA_A$ receptors, and to extend this analysis to GABAergic inhibitory postsynaptic currents (IPSCs). To this purpose, we have investigated the effect of OETX on miniature IPSCs (mIPSCs) and on current responses elicited by ultrafast GABA applications in rat cultured hippocampal neurons. We show that mIPSCs are potently inhibited by OETX, and, based on the analysis of OETX effect on current responses to rapid GABA applications, we conclude that the major mechanism of OETX action on $GABA_A$ receptors is an allosteric modulation of the binding rate and receptor desensitization with a possible contribution from open channel block.

Methods

Isolation of OETX (Figure 1)

Dried underground parts of *Oenanthe crocata* (95 g) were extracted with acetone (2 × 1 L) to afford 3.1 g of a brownish oil, which was directly purified by flash chromatography (Biotage SP1 system on a silica gel (10 g) column (FLASH 12+M type, Biotage, Uppsala, Sweden) using an *n*-hexane-ethyl acetate gradient of increasing polarities (flow rate 9 mL·min^{-1}; UV detector: 316 nm; fractionation mode: volume, 9 mL per fraction). Fractions 29–31 (*n*-hexane- ethyl acetate, 6:4) afforded 88 mg OETX (Figure 1) as a colourless foam that could not be stored in this form. However, solutions in hydrocarbon solvents (benzene, toluene) or DMSO could be stored for at least 6 months at 4°C without any apparent degradation (by ^{1}H NMR analysis) or development of the reddish colour typical of the degradation of polyacetylenes. OETX was identified by comparison with its reported spectroscopic data (Appendino *et al.*, 2009). For the electrophysiological experiments, a stock solution of OETX was prepared by dissolving it in DMSO at a final concentration of 10 mM. OETX was tested in concentrations up to 10 μM, and therefore the maximum DMSO concentration was 0.1%. In all these experiments, the OETX solvent (DMSO) was present at the same concentration in control and in OETX-containing solutions.

Neuronal primary cell culture

All animal care and experimental procedures were in agreement with the Polish Animal Welfare Act and had been approved by a Local Ethical Commission. Primary cell cultures of hippocampal neurons were prepared as previously described (Andjus *et al.*, 1997). Briefly, P2–P4 old Wistar rats were killed by decapitation. Hippocampi were dissected from the brain, sliced, treated with trypsin, mechanically dissociated and centrifuged twice at 40× *g*, plated in the Petri dishes and cultured. Experiments were performed on cells cultured for 9–16 days.

Electrophysiological recordings

All experiments were performed at room temperature (22–24°C). Currents were recorded in the outside-out or in the whole-cell configuration of the patch clamp technique using the Axopatch 200B amplifier (Molecular Devices Corporation, Sunnyvale, CA, USA) at −40 mV. The intrapipette solution contained: 137 mM CsCl, 1 mM $CaCl_2$, 2 mM $MgCl_2$, 11 mM BAPTA (tetra cesium salt), 2 mM ATP and 10 mM HEPES, pH 7.2 with CsOH. The composition of the external solution was the following: 137 mM NaCl, 5 mM KCl, 2 mM $CaCl_2$, 1 mM $MgCl_2$, 20 mM glucose and 10 mM HEPES, pH 7.2 with NaOH. mIPSCs were recorded in the whole-cell configuration in the gap-free mode (mIPSC recordings), and these signals were low-pass filtered with Butterworth filter at 3 kHz, and sampled at 10 kHz using the analogue-to-digital converter Digidata 1322A (Molecular Devices Corporation). The current responses to rapid GABA applications (especially at high GABA concentrations) required a higher time resolution and were filtered at 10 kHz and sampled at 50–100 kHz. For acquisition and signal analysis, pClamp 10.1 software was used (Molecular Devices Corporation). Miniature synaptic currents (mIPSCs) were recorded in the presence of 1 μM of tetrodotoxin and kynurenic acid (1 mM) at a holding voltage of −40 mV. Solutions were changed by gravity through a glass tube (i.d. 1 mm) directly onto the recording area with a flow of about 2 mL·min^{-1}. This system allowed the drug concentration to be reliably controlled in the surrounding of neurons from which the recordings were made. The recovery of mIPSCs after OETX treatment was slow, and for this reason washing of the cells after application of OETX was extended to at least 10 min. Cells exhibiting rundown of the mIPSC amplitude larger than 20% during the entire recording period were excluded from the analysis. For the whole-cell recordings, pipette resistance (electrodes filled with the internal solution) was 2–3.5 MΩ. Access resistance was monitored and typically compensated at 30–80%. Cells exhibiting access resistance larger than 15 MΩ (after compensation) were rejected. Current responses to 3 μM GABA were barely detectable in the excised patch configuration (especially following OETX treatment), and for this reason were recorded in the whole-cell mode using a multibarrel system (RSC-200, Bio-Logic, Grenoble, France, exchange time approximately 15–50 ms).

Rapid drug application

GABA was applied to excised (nucleated) patches using the rapid perfusion system based on a piezoelectric-driven theta-glass application pipette (Jonas, 1995). The theta-glass tubing was from Hilgenberg (Malsfeld, Germany), and the piezoelec-

tric translator was from Physik Instrumente (preloaded HVPZT translator 80 μm, Waldbronn, Germany). The open tip recordings of the liquid junction potentials have shown that 10–90% exchange of solution occurred within 50–80 μs. In experiments in which the effect of OETX was examined, the drug was present at the same concentration in solutions supplied by both channels (wash and GABA-containing solution) of the theta-glass capillary. Before applying the agonist (in the presence or absence of OETX), the patch was exposed to the washing solution for at least 2 min. In some recordings, a briefer OETX pretreatment (approximately 1 min) was applied, and the effect of OETX was very similar to that observed after 2 min, implying that pretreatment time within the range of minutes was not critical. The data included in the statistics were obtained after 2 min pretreatment.

In order to avoid excessive accumulation of OETX in the recording chamber (30 mm Petri dish), in all the electrophysiological experiments, the cells were superfused with fresh Ringer solution at the rate of 2 mL·min^{-1}.

Data analysis

The onset kinetics of currents was quantified as 10–90% rise time (RT). Deactivation of current responses (time-course after agonist removal) or the decaying phase of mIPSCs was fitted with a sum of two exponents: $y(t) = A_1 \exp(-t/\tau_{fast}) + A_2 \exp(-t/\tau_{slow})$ where A_1 and A_2 are the amplitudes of respective components, while τ_{fast} and τ_{slow} are the time constants. For normalized currents, $A_1 + A_2 = 1$. The mean deactivation or decay time constant was calculated as $\tau_{mean} = A_1\tau_{fast} + A_2\tau_{slow}$. The desensitization kinetics was described by a sum of one exponential function and a constant value representing the steady-state current ($y(t) = A \exp(-t/\tau_{Des}) + C$). The effect of OETX on mIPSCs or on current responses was assessed from the comparison between control and test recordings obtained from the same neuron (or excised patch). For this reason, the results are presented as relative values normalized to the respective controls.

As OETX strongly reduced the mIPSC amplitudes, we have tentatively applied the count matching procedure (Stell and Mody, 2002). This method corrects for the error resulting from missed mIPSCs that, due to decreased amplitude, were not resolved out of the baseline noise. In practice, using this procedure, the population of all mIPSCs recorded in the presence of OETX was compared with the subpopulation of the largest control mIPSCs matching the same number of events.

The total charge transfer per time unit was calculated as the product of averaged charge transfer for individual mIPSC and frequency of mIPSC occurrence.

Data are expressed as mean ± SEM, and paired Student's *t*-test was used for data comparison, and differences were considered significant when $P < 0.05$.

Results

OETX strongly inhibits GABAergic mIPSCs

The effect of OETX was first assessed on the amplitude of mIPSCs. In control conditions, the mIPSC amplitude (measured at –40 mV) was –36.4 ± 2.7 pA ($n = 35$). Addition of OETX to the extracellular solution resulted in a clear amplitude reduction in a concentration-dependent manner (Figure 2A,B). A significant mIPSC amplitude decrease was observed at OETX concentration as low as 0.03 μM, and the IC_{50} value was estimated to be approximately 0.35 μM. OETX-induced reduction of mIPSC amplitude was accompanied by a decrease in synaptic current frequency, which in control conditions was 0.46 ± 0.04 Hz ($n = 32$, Figure 2C). mIPSCs were measured at –40 mV because of good stability of recordings at this voltage, but we have additionally tested the impact of 0.03 μM OETX on mIPSC frequency and amplitude at –70 mV, and found no difference with respect to OETX effects observed at –40 mV (data not shown). It is noteworthy that the concentration dependence of the effect of OETX on mIPSC amplitude (Figure 2B) was unusual – it did not show a typical sigmoidal relationship, and at OETX concentrations above 0.3 μM, mIPSC amplitude steeply decreased with toxin concentration, becoming undetectable above 0.5 μM. For this reason, the IC_{50} value was not extracted from any 'logistic equation' fitting, but from linear interpolation between data points corresponding to OETX concentrations of 0.3 and 0.5 μM. As the decrease in mIPSC amplitude was associated with frequency reduction, we have tentatively applied the count matching procedure (Stell and Mody, 2002, see Methods) that yielded a concentration dependence shown in Figure 2D. However, it needs to be stressed that in the case of OETX, the use of this approach should be made with caution, as we cannot assume that the observed reduction of mIPSC frequency is solely due to 'hiding' small mIPSCs in the baseline noise (and not, for instance, from a presynaptic action). In order to see whether OETX affected preferentially mIPSCs with large or small amplitudes, the cumulative distributions for controls and 0.03, 0.1, 0.3 μM OETX were constructed (Figure 2E). The fact that distributions in control conditions and in the presence of OETX appear roughly parallel indicates that there is no obvious dependence of toxin potency on mIPSC amplitude.

OETX affects the mIPSC kinetics

The charge transfer of an individual mIPSC depends not only on current amplitude, but also on its duration, and for this reason it is important to analyse the impact of OETX on the mIPSC kinetics. As OETX strongly reduced mIPSC amplitudes, kinetic analysis was feasible for toxin concentrations up to 0.3 μM. The analysis of OETX effect on synaptic current time-course was performed on averaged mIPSCs, and the impact of the toxin was assessed from comparison of data obtained in control conditions and in the presence of OETX on the same neuron (i.e. relative values are reported). In control conditions, the 10–90% RT of mIPSC was 1.08 ± 0.09 ms ($n = 22$). Addition of OETX to the external solution clearly slowed the mIPSC onset kinetics (Figure 3A,B). The time duration of mIPSC is largely determined by its decaying phase. In control conditions, this phase of the synaptic current could be well fitted with a biexponential function characterized by the following parameters: $A_1 = -14.64 \pm 1.57$ pA, $A_2 = -18.15 \pm 1.71$ pA, $\tau_{fast} = 13.37 \pm 1.00$ ms, $\tau_{slow} = 72.35 \pm 6.08$ ms, $\tau_{mean} = 39.63 \pm 1.90$ ms, for normalized currents $A_1 = 0.44 \pm 0.03$, $n = 31$. Application of OETX resulted in a clear acceleration

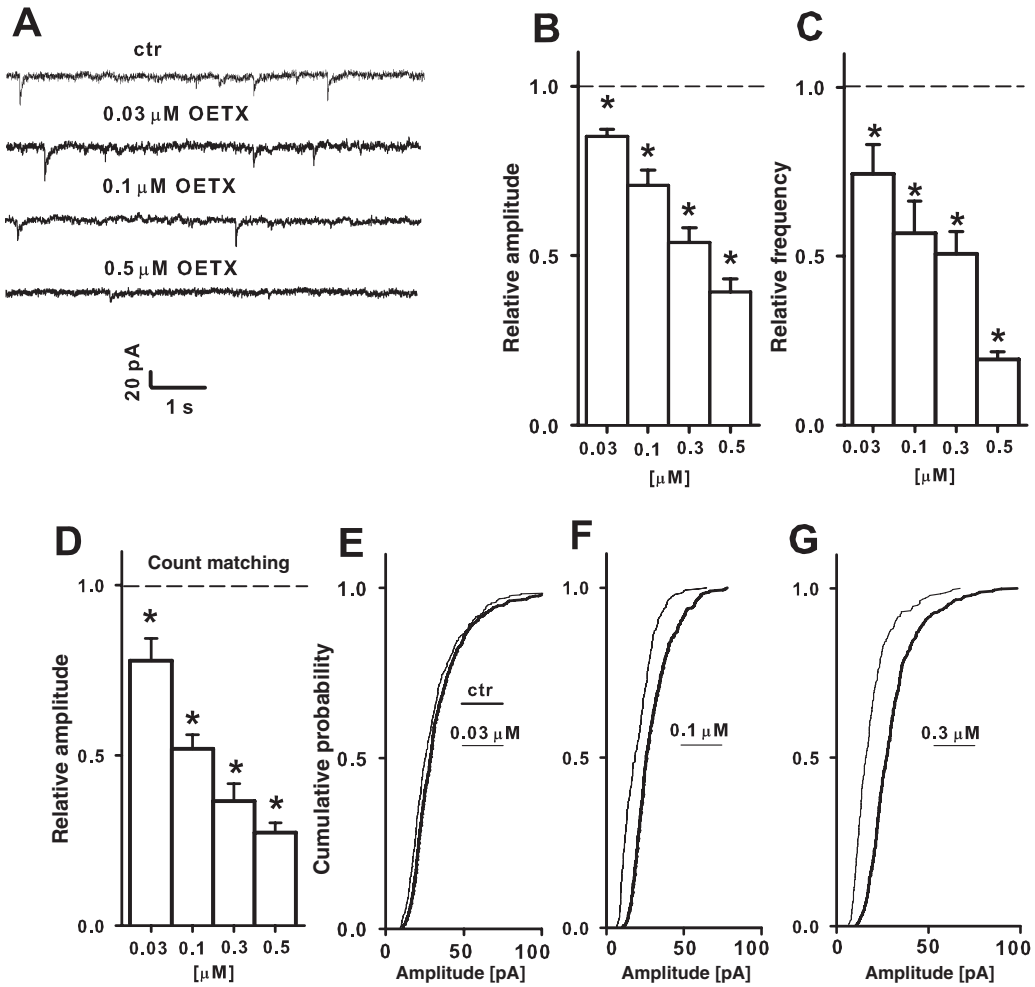

Figure 2 OETX strongly inhibits amplitude of the mIPSCs. (A) Examples of mIPSCs recorded at −40 mV in control conditions (upper trace) and in the presence of OETX at concentrations indicated above the traces. (B, C) Summary results of OETX on mIPSC amplitudes (B) and frequency (C). Each value of amplitude or frequency was normalized to the value obtained in control conditions for the same cell. (D) Summary results of OETX on mIPSC amplitudes calculated using the count matching procedure (Stell and Mody, 2002). (E–G) Cumulative histograms constructed for all mIPSC amplitude values measured at the OETX concentrations indicated on the graphs and controls, measured from the same neurons. Bars represent averaged relative values determined at the OETX concentrations shown. The averaged values reported in the graphs were calculated from at least four cells. Dashed lines indicate unitary relative values corresponding to the control conditions. *$P < 0.05$, significantly different from controls.

of the mIPSC decaying phase (Figure 3C,D). This effect was associated with a decrease in both slow and fast time constants, although at 0.3 μM OETX, there was no effect on the latter (Figure 3E,F). Besides its effect on the time constant, OETX reduced the percentage of the slow component by 30–55% for the considered range of OETX concentrations, but due to the wide scatter of these data, the changes did not reach statistical significance (data not shown).

Analysis of the effect of OETX on GABAergic synaptic currents shows that the total charge transferred by mIPSCs is strongly diminished by this toxin because of reduction of current amplitude (Figure 2A,B), frequency (Figure 2C) and decaying phase (Figure 3C,D). When considering all these effects together, the effect of OETX on the total charge transfer can be determined (Figure 3G). Importantly, such an overall effect of OETX on charge transfer is particularly strong as a toxin concentration of less than 0.03 μM halved the charge transfer.

Effect of OETX on current responses to exogenously applied GABA

The mechanism of any modulation of $GABA_A$ receptors cannot be determined based solely on the analysis of its effect on the synaptic currents. Although the averaged peak of synaptic GABA concentration and the time-course of its clearance can be estimated (Clements *et al.*, 1992; Clements, 1996; Mozrzymas *et al.*, 1999; 2007; Overstreet *et al.*, 2002; Mozrzymas, 2004), a thorough pharmacological analysis requires concentration–response relationships (i.e. experimental protocols controlling the applied agonist concentration and time-course). It needs also to be taken into consideration that synaptic GABA transients are very fast (time duration of hundreds of microseconds: Clements, 1996; Mozrzymas *et al.*, 1999; 2007; Overstreet *et al.*, 2002; Mozrzymas, 2004), while the activation kinetics of $GABA_A$ receptors at high GABA concentrations occurs within a submillisecond time-scale (Maconochie *et al.*, 1994; Jones and Westbrook, 1995;

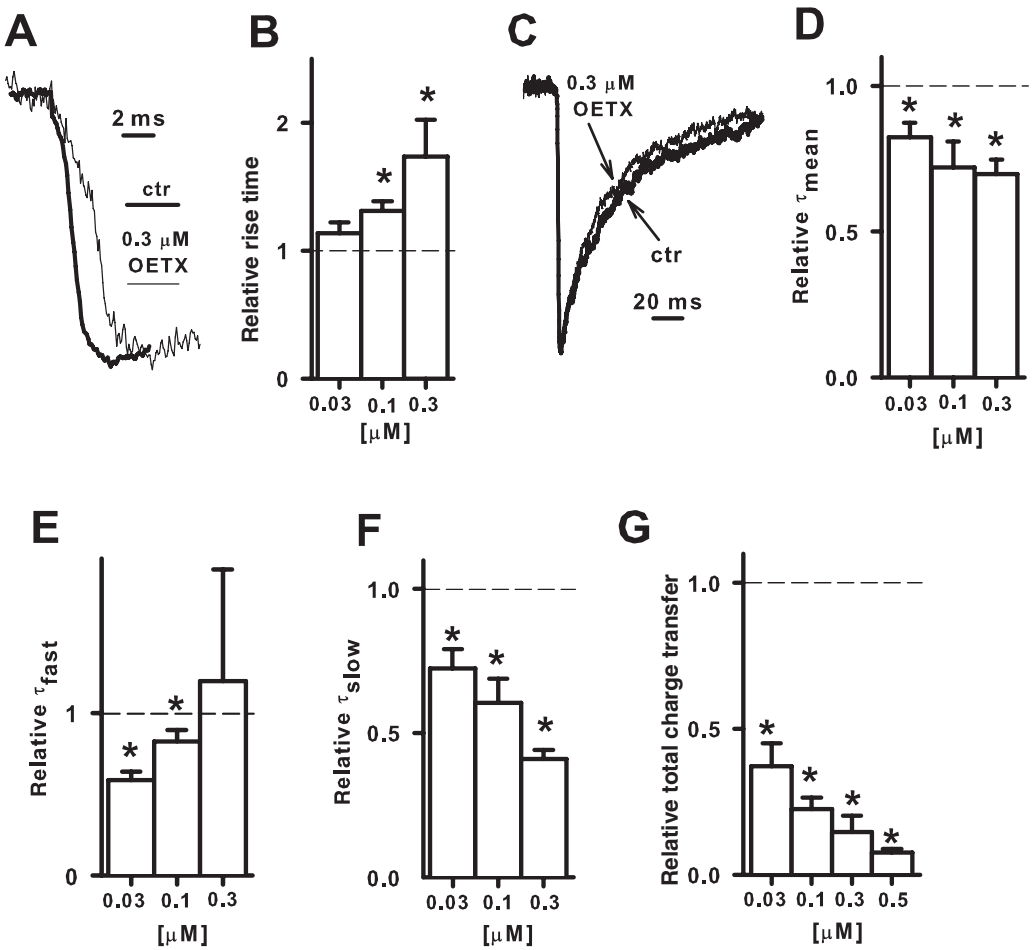

Figure 3 OETX affects the mIPSC time-course. (A) Typical normalized rising phases of averaged mIPSCs measured from the same cell in control conditions and in the presence of 0.3 μM OETX. Note that OETX slows the onset rate of mIPSC. (B) Summary results of OETX on the mIPSC 10–90% RT (values relative to controls are presented). (C) Typical normalized mIPSCs in control conditions and in the presence of 0.3 μM OETX. Note that OETX accelerates the decaying phase of mIPSC. (D) Summary results of OETX on the decaying phase of mIPSC (assessed as τ_{mean}, values relative to controls). (E, F) Summary results of OETX on the fast and slow time constants (τ_{fast}, τ_{slow}). (G) Summary results of OETX on the total charge transfer. Note that due to a cumulative OETX effect on mIPSC amplitude, frequency and decaying phase, the relative value of the total charge transfer falls below 0.5 at OETX concentration as low as 0.03 μM. Bars represent averaged relative values determined at the OETX concentrations shown. The averaged values reported in the graphs were calculated from at least four cells. Dashed lines indicate unitary relative values corresponding to the control conditions. *$P < 0.05$, significantly different from controls.

Mozrzymas *et al*., 2003a). Taking this into account, the binding and gating properties of these $GABA_A$ receptors need to be studied with adequate time resolution that can be achieved with an ultrafast application system (Jonas, 1995).

Effect of OETX on current responses elicited by low GABA concentration (3 μM) indicates a complex blocking mechanism

Currents evoked by 5 s application of 3 μM GABA were recorded in the whole-cell configuration at –40 mV. At this GABA concentration, the current kinetics are relatively slow, and it was sufficient to apply the agonist using the multibarrel RSC-200 Bio-Logic system (see Methods). OETX clearly reduced the amplitude of currents in a concentration-dependent manner (Figure 4A,B). Tentatively, we have fitted to the concentration–response relationship presented in Figure 4B using the sigmoidal 'logistic equation' in the form of Equation 1, where [*OETX*] is the toxin concentration, and *h* is the Hill's coefficient, and the estimated half-blocking OETX concentration was 0.1 μM.

$$y(t) = \frac{1}{(1 + [OETX] \cdot \mathrm{IC}_{50}^{-1})^{h}} \quad (1)$$

This fit was used only as a technical tool to extract the approximate value of IC_{50}, as the use of such logistic equations has important limits (see Mozrzymas *et al*., 2003a for a more detailed discussion related to this point). Interestingly, although OETX concentration above 0.5 μM practically abolished the mIPSCs (Figure 2), for responses to 3 μM GABA, measurable currents could be still observed even at OETX concentrations higher than 3 μM (Figure 4B).

Current responses to 3 μM GABA within the time-scale of 5 s show a relatively weak fading that is commonly attributed to receptor desensitization (Figure 4A, trace on the left-hand side). Interestingly, in the presence of relatively low OETX concentrations, the current fading appeared deeper within

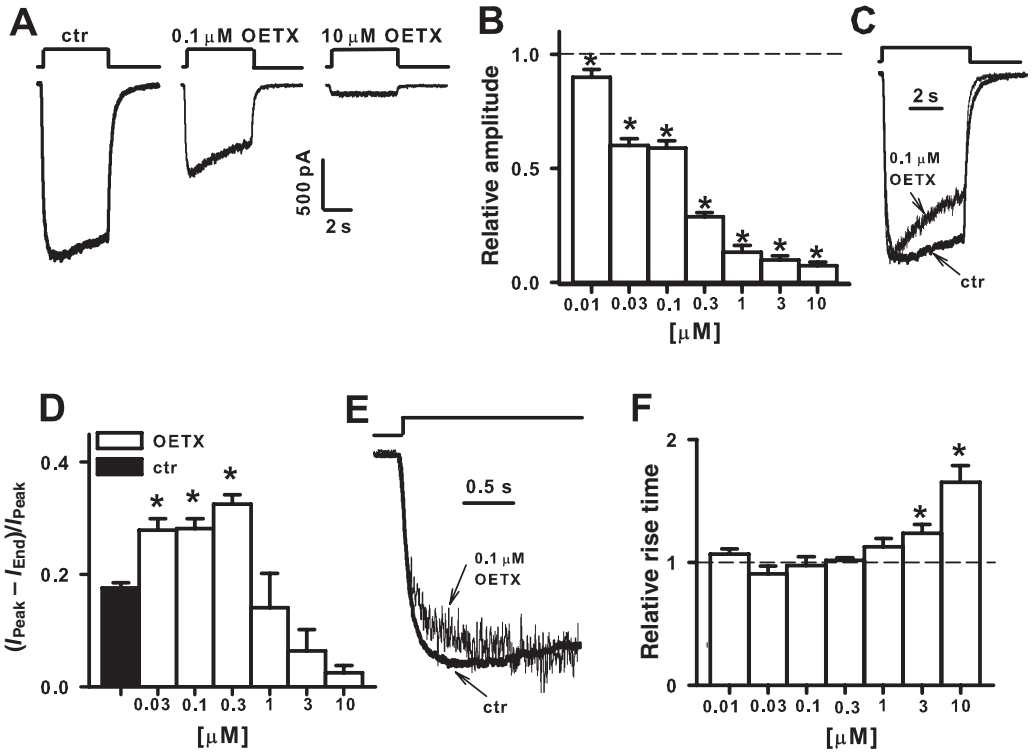

Figure 4 OETX inhibits current responses to low (3 μM) GABA concentrations, and alters their time-course. (A) Typical traces of currents elicited by application of 3 μM GABA in control conditions (left) and in the presence of OETX at concentrations indicated above the current traces. (B) Concentration–response relationship for OETX effect on current amplitude. (C) Normalized and superimposed current traces recorded in control conditions and in the presence of 0.1 μM OETX. Note that OETX at this concentration enhances the fading phase. (D) Statistics of the extent of fading assessed as $(I_{peak} - I_{End})\cdot I_{peak}^{-1}$, where I_{peak} is the peak value of current, I_{End} is the current value at the end of 5 s GABA application. Note that at low OETX concentrations, fading increases, but at higher OETX doses tends to disappear. (E) Typical normalized and superimposed current traces recorded in control conditions and in the presence of 10 μM OETX. (F) Summary results of OETX on the rising phase of currents evoked by 3 μM GABA. Note that a statistically significant effect was observed only at highest OETX concentration (3, 10 μM). All the insets above the current traces indicate the duration of 3 μM GABA application. Bars represent averaged relative values determined at the OETX concentrations shown. The averaged values reported in the graphs were calculated from at least seven cells. Dashed lines indicate unitary relative values corresponding to the control conditions. *$P < 0.05$, significantly different from controls.

the same time window (see Figure 4C). The extent of fading within 5 s agonist application was quantified using the parameter: $(I_{Peak} - I_{End})\cdot I_{Peak}^{-1}$, where I_{Peak} is the current peak amplitude and I_{End} is the current value at the end of 5 s GABA application. For OETX concentrations within the range 0.03–0.3 μM, the extent of fading was enhanced by this toxin, while at higher concentrations, current fading tended to disappear (Figure 4D).

The enhancement of current fading in the presence of OETX might result from a variety of mechanisms including open channel block (as with picrotoxin, Newland and Cull-Candy, 1992) or an allosteric modulation of the receptor kinetics. To distinguish between different possibilities, we analysed the effect of OETX on additional parameters describing the current time-course. At low OETX concentration, the 10–90% RT was not affected, while at higher toxin doses, it was clearly slowed (Figure 4E,F). A pure open channel blocker would be expected either not to affect the current onset or to accelerate it. Such acceleration of current onset would be expected when the rate of current onset is comparable to that of channel block (this could occur at a low agonist concentration at which a slowly rising response would be 'trimmed' by the antagonist-mediated blockade). Taking into account this prediction, the observed slow-down of the onset kinetics at higher OETX concentrations indicates that open channel block cannot be the only mechanism underlying the current block.

Inhibition of responses to 3 μM GABA by OETX at –40 and +40 mV did not show any significant difference, indicating that at least for currents evoked by low GABA concentrations, the blocking effect of OETX was not voltage dependent.

OETX strongly slows the onset of currents evoked by an intermediate GABA concentration (30 μM)

In order to further explore the mechanism of OETX action on $GABA_A$ receptors, we have examined the effect of this compound on current responses evoked by a GABA concentration close to the EC_{50} value, at which the modulation of agonist binding kinetics is expected to have a marked impact both on current amplitude and the onset kinetics (see Mozrzymas *et al.*, 2003a). To this end, we have checked the effect of OETX on currents elicited by 30 μM GABA. The application time of GABA was set at 100 ms that was sufficient for the current response to reach its peak value both in control conditions and in the presence of OETX. In control conditions, the

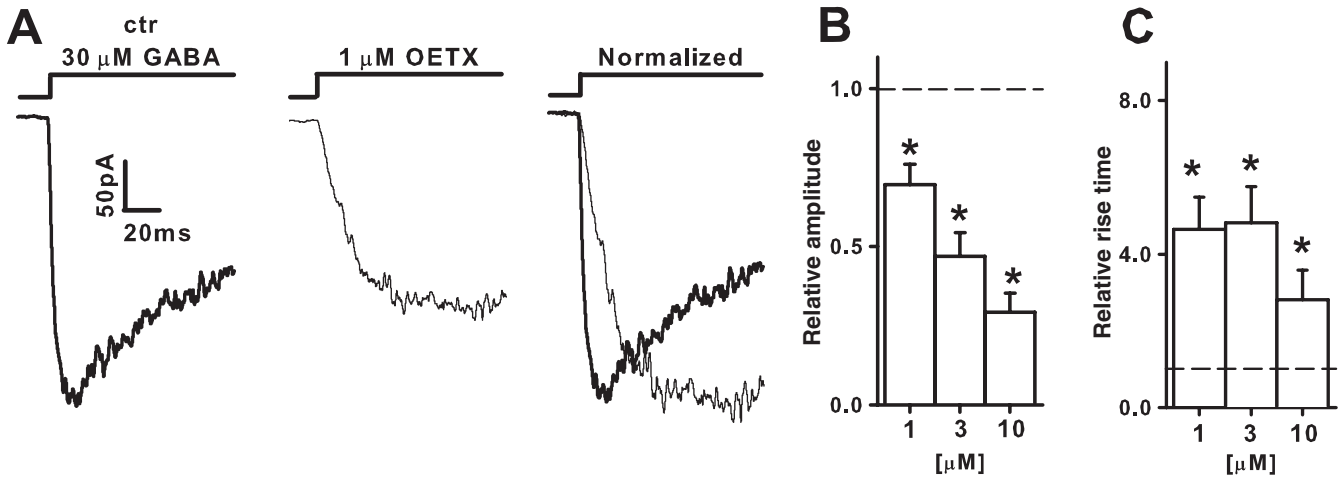

Figure 5 OETX strongly slows down the onset rate and reduces the amplitude of current responses evoked by 30 μM GABA. (A) Typical current response to 30 μM GABA (left), current response to the same GABA concentration in the presence of 1 μM OETX (middle) and normalized and superimposed current traces in control conditions and in the presence of 1 μM OETX (right). Note that OETX-induced reduction of the onset rate is particularly strong. (B) Summary results of OETX on the current amplitude (relative to controls). (C) Summary results of OETX on the 10–90% RT calculated relative to control values. Insets above the current traces indicate application time of 30 μM GABA. Bars represent averaged relative values determined at the OETX concentrations shown. The averaged values reported in the graphs were calculated from at least eight cells. Dashed lines indicate unitary relative values corresponding to the control conditions. *$P < 0.05$, significantly different from controls.

10–90% RT of current evoked by 30 μM GABA was 11.9 ± 1.3 ms (n = 33). As shown in Figure 5A,B, OETX reduced the amplitude of these currents in a concentration-dependent manner. Interestingly, the effect of OETX on current amplitudes was considerably weaker than that observed for 3 μM GABA (compare Figures 4 and 5). Interestingly, current amplitude reduction by OETX was accompanied by a strong reduction in the current onset rate (Figure 5A,C). This finding suggests that OETX might potently down-regulate the rate of binding. However, this proposal requires further evidence, as slower onset might also result from alterations in the receptor gating (conformational transitions between receptor bound conformations).

OEXT effect on current responses to saturating (GABA) reveals its impact on GABAAR gating kinetics

At low and intermediate GABA concentrations, time-course of evoked currents depends both on binding and gating kinetics. However, at saturating GABA concentrations, binding becomes much faster than conformational transitions between bound states, and at sufficiently high GABA concentrations, the current time-course reflects mainly the kinetics of conformational transitions (gating). To assess the effects of OETX on $GABA_A$ receptor gating, current responses to 10 mM GABA were recorded in the outside-out (nucleated) mode of the patch clamp technique at –40 mV. The duration of GABA application was set at 100 ms, enabling us to monitor in a single sweep both the onset and desensitization kinetics. Interestingly, the current response to 10 mM GABA in the presence of 1 μM OETX, recorded after respective control, was characterized by a striking biphasicity: initially a fast onset and rapid desensitization (arrows indicating insets in Figure 6A, second and third current trace) followed by a slow 'rebound' phase (Figure 6A, insets). The rapid current component has apparently similar onset kinetics to that observed in controls (see below for more detailed analysis of the onset kinetics), and thus it seems to involve a proportion of receptors that were not affected by OETX. The slow rebound phase appears thus to reflect the activity of $GABA_A$ receptors whose gating was profoundly affected by OETX. Surprisingly, when recording a subsequent current trace in the presence of OETX, the fast current component decreases, while the slow one increases (Figure 6B). Note that in our experiments with OETX, this compound was present not only in the pipette supplying GABA, but the excised patch was exposed to the washing solution containing OETX for at least 2 min before GABA application (see Methods). This means that receptor exposure to OETX lasting for at least 2 min is insufficient complete its inhibitory effect in the absence of GABA, while relatively brief (100 ms) co-exposure of toxin with GABA produces additional block of the fast component, perhaps indicating the involvement of open channel block. Interestingly, the increased inhibition of the fast component observed in the second pulse is accompanied by an increase in the amplitude of the slow component (Figure 6B). Two subsequent pulses were sufficient to stabilize the amplitude of both rapid and slow current components, and thus, to construct the concentration–response relationship, we have considered the second response recorded in the presence of OETX. As shown in Figure 6C, OETX reduced current responses to 10 mM GABA, but again its effect appears smaller than that obtained for 3 μM GABA or for mIPSCs (compare concentration–response relationships in Figures 4 and 6C, and that for synaptic currents, Figure 2). As OETX might decrease the binding affinity of $GABA_A$ receptors (see above the analysis of responses to 30 μM GABA), 10 mM GABA, in the presence of OETX, could be insufficient to saturate the response. To test this possibility, the effect of OETX was additionally tested for responses to 30 mM GABA. However, the effects of this toxin

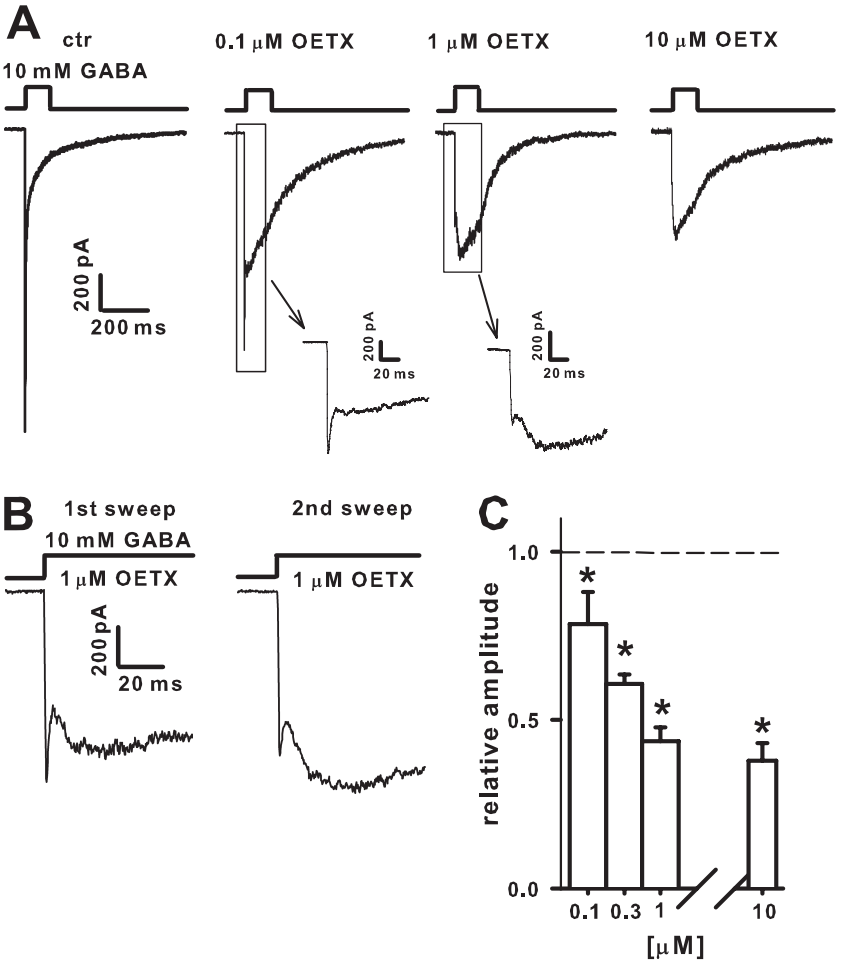

Figure 6 OETX reduces the amplitude and alters the time-course of current responses evoked by saturating (10 mM) GABA concentration. (A) Typical current responses to 10 mM GABA applied for 100 ms recorded in control conditions (left) and in the presence of 0.1, 1 and 10 μM OETX (successive traces). Note that currents recorded in the presence of 0.1 and 1 μM OETX were characterized by a rapid and slow components (see insets). (B) Typical consecutive current responses evoked by a saturating GABA concentration (10 mM, 100 ms) in the presence of 1 μM OETX. Note that in the second sweep, the rapid component is diminished with respect to the slow one while the slow component increased. (C) Concentration–response relationship for amplitudes of current responses evoked by saturating GABA (10 mM, 100 ms) applications (second sweeps were considered). All the insets above the current traces indicate the duration of 10 mM GABA application. Bars represent averaged relative values determined at the OETX concentrations shown. The averaged values reported in the graphs were calculated from at least four cells. Dashed lines indicate unitary relative values corresponding to the control conditions. *$P < 0.05$, significantly different from controls.

on current amplitudes and onset kinetics did not show any significant difference with respect to those observed for response elicited by 10 mM GABA (data not shown).

As OETX exerted a complex effect on the onset kinetics of currents evoked by 10 mM GABA, particular care was taken to analyse this parameter. In control conditions, the 10–90% RT of current evoked by 10 mM GABA was 0.69 ± 0.04 ms (nucleated patches, $n = 41$). As already mentioned, at low OETX concentrations, the rapid onset component was predominant, and its 10–90% RT was apparently identical to that in controls (Figure 7A,B). However, when the amplitude of the rapid component was smaller than the slow one, the same algorithm for calculating the onset kinetics could indicate the 10–90% RT of slow component (Figure 7C). For this reason, when applying the 10–90% criterion for the entire rising phase of the current response, the onset kinetics showed a particular concentration–response characterized by a robust increase in 10–90% RT value above 1 μM OETX (Figure 7D, second GABA application was considered in the statistics). Such a large increase in 10–90% RT value was caused by the fact that above 1 μM OETX, the slow component was predominant in all cells assayed. Taking into account such a biphasicity of the current onset kinetics related to the action of OETX, an attempt was made to analyse the RT kinetics for the two components separately. When restricting the onset analysis to the second GABA application (in the presence of OETX), the fast component was detectable for OETX concentration up to 1 μM, and, as it is shown in Figure 7E, the toxin had no significant effect on the 10–90% RT of this component. In the case of 10–90% RT kinetics of the slow current component, it is important to note that only time at 90% of its peak value can be measured, while the 10% value cannot, as the two phases of currents overlap (Figures 6 and 7). However, determination of the 10% value from the rapid

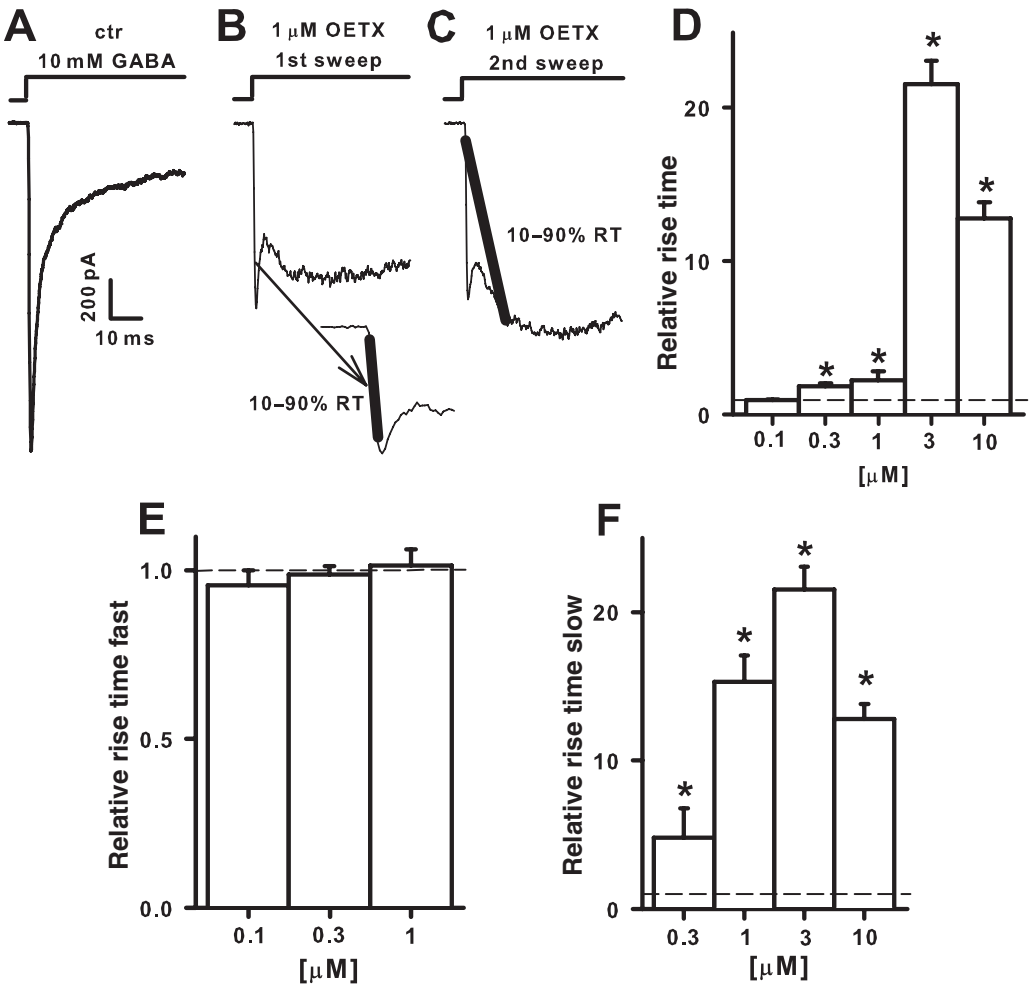

Figure 7 OETX affects the rising phase kinetics of current responses to saturating GABA concentrations. (A) Typical control current response evoked by 10 mM GABA. (B) Example of current evoked by 10 mM GABA in the presence of 1 μM OETX in which the amplitude of the fast component is larger than the slow one. In such a case, the standard procedure for 10–90% RT would be applied to the fast component (see inset). (C) Example of current evoked by 10 mM GABA in the presence of 1 μM OETX in which the amplitude of the fast component is smaller than that of the slow one. In this case, the 10–90% RT would be applied to the slow component (see inset) yielding the 10–90% RT value much larger than in the case presented in B. (D) Summary results of OETX on the 10–90% RT determined as shown in B and C (the second GABA application was used for analysis). (E) Summary results of OETX on RT of the fast component of current response to 10 mM GABA. (F) Summary results of OETX on the 10–90% RT of the slow component of current evoked by 100 ms application of 10 mM GABA. All the insets above the current traces indicate the duration of 10 mM GABA application. Bars represent averaged relative values determined at the OETX concentrations shown. The averaged values reported in the graphs were calculated from at least five cells. Dashed lines indicate unitary relative values corresponding to the control conditions. *$P < 0.05$, significantly different from controls.

component is expected to produce only a minor overestimation of the 10–90% RT value of the slow component. As presented in Figure 7F, the values of 10–90% RT for the slow current component show that the current rising phase was dramatically increased by OETX with respect to control conditions. These data on OETX effect on current responses to saturating GABA concentrations taken together indicate that OETX affects $GABA_A$ receptor gating.

Desensitization is known to critically shape both the kinetics and amplitudes of GABAergic currents (Jones and Westbrook, 1995; Mozrzymas *et al.*, 2003b; 2007) and can be visualized as the decaying phase of currents elicited by rapid application of saturating agonist (Figure 8A). At OETX concentrations at which the rapid current component shown in Figures 6A and 7B,C (presumably due to $GABA_A$ receptors not affected by OETX) is either small (minimally influencing the peak current) or no longer present (3, 10 μM), currents are characterized by a weak current fading following the peak indicating that OETX has largely abolished the rapid component of the desensitization process (Figure 8A, right).

We have additionally checked whether OETX affected the deactivation kinetics. As deactivation strongly depends on the duration of application of saturating GABA concentrations (Mozrzymas, 2004; Mozrzymas *et al.*, 2007), the agonist application time had to be set equal for controls and OETX-treated neurons. In an attempt to draw an analogy with synaptic currents, our initial trials were made for current responses evoked by brief agonist pulses (1–3 ms, Figure 8B), and in these conditions, at high OETX concentrations the amplitude reduction was larger than that observed for long (100 ms) GABA applications (compare Figures 6C and 8C). Such amplitude reduction was accompanied by an acceleration of the

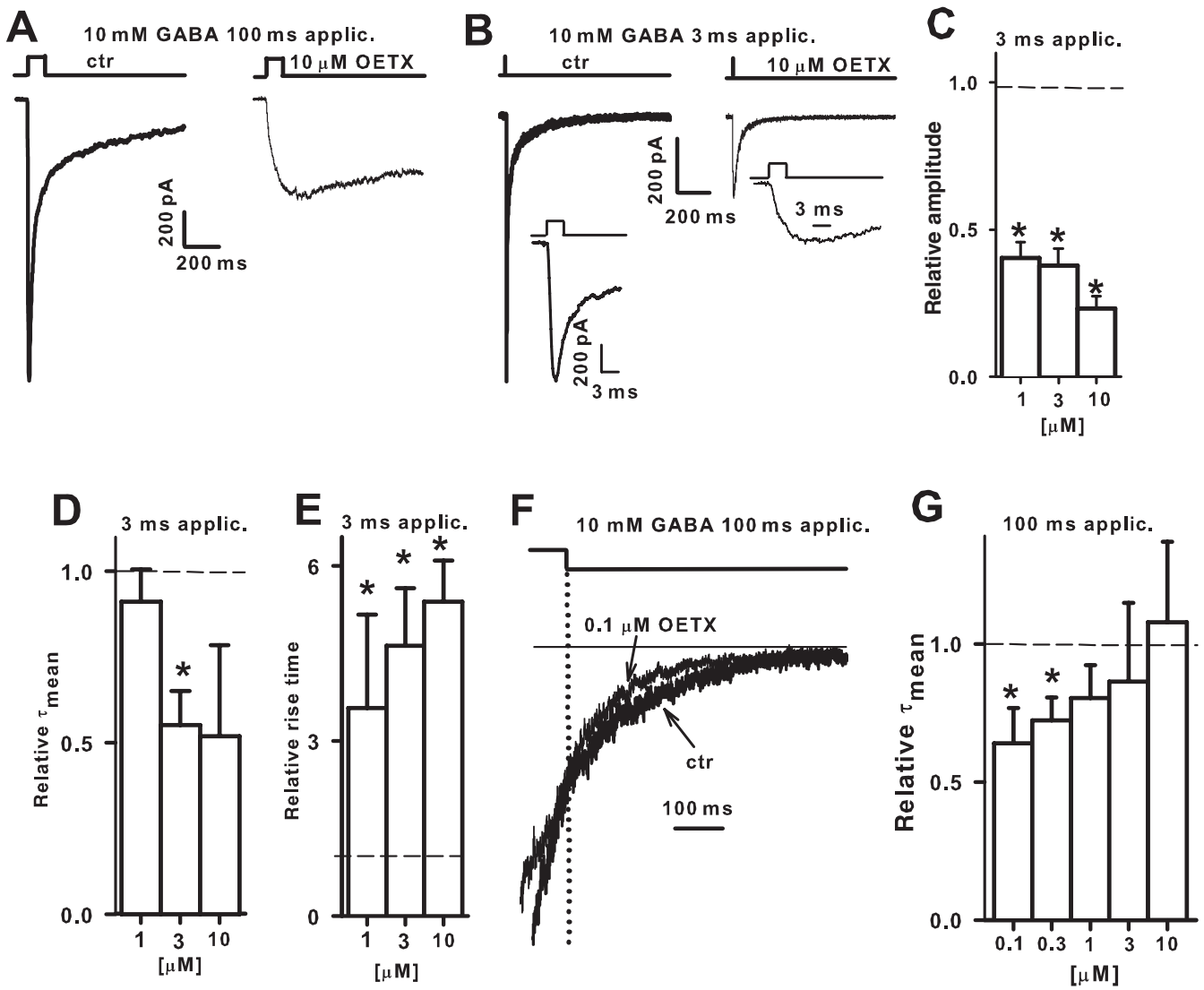

Figure 8 OETX affects the desensitization and deactivation kinetics of currents evoked by saturating GABA concentrations. (A) Typical current responses to prolonged application of 10 mM GABA in control conditions (left) and in the presence of 10 μM OETX (right). Note that the current fading due to desensitization onset in (A, right) has almost disappeared in the presence of 10 μM OETX. (B) Typical current responses evoked by a short (3 ms) application of 10 mM GABA in control conditions (left top) and in the presence of 10 μM OETX (right top). The current traces recorded in control conditions and in the presence of 10 μM OETX were additionally presented in the expanded time-scale (A, left bottom and B, right bottom) to show that in the presence of OETX, the rising phase kinetics outlasts the agonist application (inset), while the peak of control current occurs within the application of GABA. The upper amplitude scale bar is valid for all the current traces except for that shown in left bottom (control recording in the expanded time-scale). (C, D) Summary results of OETX on amplitude (C) and deactivation kinetics measured as τ_{mean} (D) of current responses evoked by short (3 ms) applications of saturating GABA. (E) Summary results of OETX on the 10–90% RT for current responses evoked by short application of 10 mM GABA. Note that in spite of short duration of GABA application, the onset kinetics is prolonged several fold. (F) Typical normalized deactivation currents measured after 100 ms (dotted line indicates the moment of agonist removal) application of 10 mM GABA. The currents are normalized to the amplitude values at the moment of agonist removal. Note that OETX accelerates the deactivation kinetics of current responses. (G) Statistics of OETX effect on the deactivation kinetics (assessed in terms of τ_{mean}) for currents evoked by 100 ms application of 10 mM GABA. Note that at low OETX concentrations (0.1, 0.3 μM), the deactivation kinetics is accelerated by this toxin. All the insets above the current traces indicate the duration of 10 mM GABA application. Bars represent averaged relative values determined at the OETX concentrations shown. The averaged values reported in the graphs were calculated from at least three cells. Dashed lines indicate unitary relative values corresponding to the control conditions. *$P < 0.05$, significantly different from controls.

deactivation kinetics (Figure 7D), but in these conditions (short GABA application), the slow rebound-like phase (see Figure 6A) was not observed in the majority of recordings (15 out of 17 recordings in the presence of OETX), while in two recordings there was only a slight slow phase (data not shown). These findings are consistent with observations described above that within first milliseconds of GABA applications, the receptors not affected by OETX are likely to contribute to the rapid onset phase of current response. However, the current responses to brief (1–3 ms) GABA applications (10 mM) are still substantial at high OETX concentrations (3 and 10 μM), although smaller than those evoked by GABA

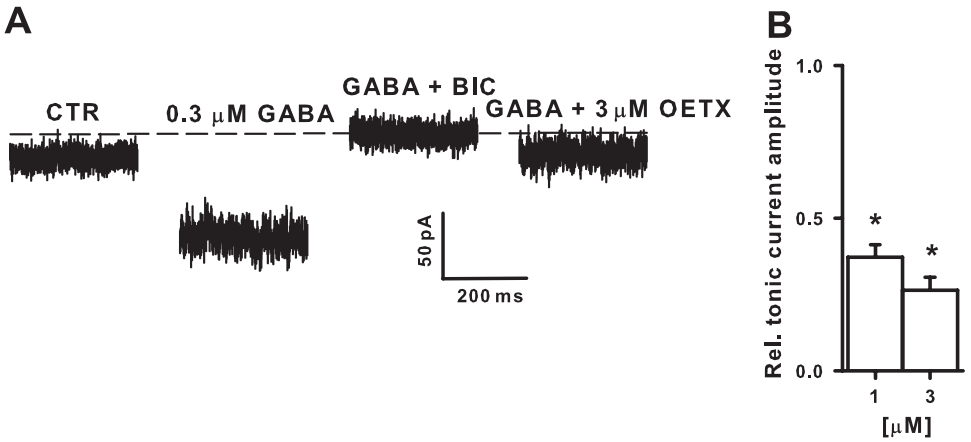

Figure 9 OETX blocks the tonic current. (A) Typical whole-cell recordings of currents are shown when superfusing the cell with normal (nominally GABA-free Ringer solution, CTR), when artificially enhancing the tonic current by application of 0.3 μM GABA (0.3 μM GABA), when co-applying 0.3 μM GABA and 30 μM bicuculline (GABA + BIC) and when co-applying 0.3 μM GABA and 3 μM OETX. The tonic current was assessed as difference between current evoked by 0.3 μM GABA with respect to the baseline measured in the presence of GABA and bicuculline (GABA + BIC). Note that when washing the cell with normal Ringer solution, a component of bicuculline-sensitive GABAergic (tonic) current was present (trace below 'CTR'), but it was too small to reliably assess the blocking effect of OETX. (B) Summary results of OETX-induced block of tonic current. Bars represent averaged relative values determined at the OETX concentrations shown. *$P < 0.05$, significantly different from controls.

(10 mM) applied for 100 ms at the same OETX concentrations (Figures 6 and 8). Interestingly, as shown in Figure 8B (insets to the current traces recorded in control conditions and in the presence of 10 μM OETX) and E, the rising phase of current response to short GABA applications in the presence of high OETX concentration clearly outlasts GABA application (1–3 ms), while in control conditions the peak occurs within the GABA application time. This observation strongly suggests that in the presence of OETX, the onset kinetics (especially after agonist removal) is relying on conformational transitions between bound states (gating) rather than on binding.

To further elucidate the impact of OETX on deactivation kinetics, we have considered the current relaxation following 100 ms GABA application (10 mM, Figure 8F). We have found that OETX exerts a moderate effect on the deactivation kinetics, resulting in a reduction of the mean deactivation time constant (τ_{mean}), but this effect tended to disappear with increasing OETX concentration (Figure 8G). Quantitative difference in the effects of OETX on deactivation of currents evoked by short (1–3 ms, Figure 8D) and long (100 ms, Figure 8G) applications of 10 mM GABA is not surprising as prolongation of agonist applications is known to affect the deactivation mechanism due to higher occupancy of receptors in the slow desensitized states (see Mozrzymas *et al.*, 2007).

Effect of OETX on the tonic current

The results described above show that the extent of inhibition of current responses by OETX was inversely correlated with GABA concentration (Figures 4–6). This observation might suggest that OETX could exert a particularly potent effect on tonic currents. However, it needs to be stressed that the $GABA_A$ receptors underlying tonic conductance could show kinetics and pharmacology distinct from those involved in mIPSCs or receptors largely determining the current responses to high GABA concentrations (presumably containing γ subunits). In order to directly address the effect of OETX on the tonic current in our model, we have implemented the approach similar to that used by Bai *et al.* (2001). Tonic current was measured at −70 mV in the whole-cell configuration, and was assessed as the current offset after application of 30 μM bicuculline (Figure 9). To prevent the contribution of $GABA_B$ receptors, we used CGP 55845, an antagonist of these receptors, at 1 μM added to the external solution. When measuring from a neuron exposed to the washing solution containing nominally no GABA, the tonic current was very small, 19.5 ± 3.2 pA ($n = 17$), and the assessment of any inhibitory effects of OETX was problematic. For this reason, we have artificially enhanced the tonic current by application of GABA at a low concentration (0.3 μM) that is typical for ambient concentration of this neurotransmitter in the brain (Farrant and Nusser, 2005). In these conditions, the tonic current was 52.4 ± 10.5 pA ($n = 9$), and application of 1 or 3 μM OETX reduced it to 0.37 ± 0.04 ($P < 0.05$, $n = 5$) and 0.26 ± 0.04 ($P < 0.05$, $n = 4$) of control values, respectively (Figure 9).

Discussion

We have recently provided the first evidence that OETX potently inhibits current responses to exogenous GABA (Appendino *et al.*, 2009). The major finding of the present work is to extend the study of OETX on GABAergic synaptic currents (mIPSCs), and to explore the pharmacological mechanism(s) underlying inhibition of $GABA_A$ receptors by this toxin.

Distinct OETX effects on mIPSCs and current responses

We have found that OETX affected both the amplitudes and kinetics of mIPSCs and current responses. In particular, OETX

slowed down the onset kinetics both in the case of mIPSCs (Figure 3A) and in current responses (Figures 4–7). Moreover, the decaying phase of mIPSCs is accelerated by OETX (Figure 3) similarly to the deactivation process of currents evoked by 10 mM GABA (Figure 8). These similarities indicate that the blockade of mIPSCs and of current responses share similar mechanisms. However, mIPSCs appear much more susceptible to OETX block than evoked currents (compare Figures 2, 3 and 4–6). Interestingly, when considering the impact of OETX on the overall charge transfer by mIPSCs (Figure 3G), the blocking effect on synaptic currents is stronger by nearly one order of magnitude. A possible explanation for this difference is that synaptic receptors show a higher sensitivity to OETX than extrasynaptic ones that contribute to currents evoked by exogenous GABA. However, the tonic current (modelled in our study as current elicited by 0.3 μM GABA, Figure 9) appeared to be less OETX sensitive than current elicited by 3 μM GABA (Figure 4). On the other hand, OETX sensitivity of current responses decreased with GABA concentration (Figures 4–6), and at 30 μM GABA the impact of OETX appeared smaller than that on tonic currents and on responses elicited by application of 3 μM GABA (Figures 4, 5 and 9). Thus, although in our model it is difficult to assess precisely the OETX sensitivity for the tonic currents (presumably mediated by high affinity δ subunit-containing $GABA_A$Rs) and current responses to higher [GABA] (≥3 μM), it seems that the effect of OETX on these currents is comparable.

OETX effect on $GABA_A$R binding and gating: impact of synaptic GABA transient kinetics

As our data do not indicate any dramatic difference in sensitivity to OETX between synaptic and extrasynaptic $GABA_A$ receptors, the issue of nearly one order of magnitude difference between the effect on mIPSCs and current responses requires alternative explanations. It is relevant to consider specific synaptic conditions in which postsynaptic responses are believed to be evoked by very brief and non-saturating GABA transients (Clements *et al*., 1992; Clements, 1996; Mozrzymas *et al*., 1999; 2007; Overstreet *et al*., 2002; Mozrzymas, 2004). Moreover, the short duration of synaptic GABA transients makes IPSCs particularly sensitive to agents affecting agonist binding kinetics (see Mozrzymas *et al*., 1999; 2007; Mozrzymas, 2004). Our analysis of the onset kinetics of currents evoked by 30 μM GABA (Figure 5) provides an indication that OETX slows the binding rate. However, the current onset was slowed also for currents elicited by saturating GABA concentrations (at which binding is much faster than gating and the latter is expected to shape the current time-course, Figure 7) raising the possibility that in both cases (30 μM and 10 mM GABA) the underlying mechanism might involve a slowing of receptor gating rather than agonist binding. Importantly, OETX at concentration of 3 μM (at which its effect on the onset kinetics was the largest both for 30 μM and 10 mM GABA), prolonged the 10–90% RT of currents evoked by 10 mM GABA by approximately 10 ms (average RT for currents evoked by 10 mM GABA in the presence of 3 μM OETX – 10.90 ms, see also Figure 7 for relative values). As 10 mM GABA is saturating, this slowing of the current onset was attributed to an effect of OETX on $GABA_A$ receptor gating. However, this change in gating properties is insufficient to explain an OETX-induced increase in the 10–90% RT from 11.9 to 55 ms (averaged values) for currents elicited by 30 μM GABA, indicating that OETX slows both binding and gating of the $GABA_A$ receptors. Consequently, OETX-induced reduction of the agonist binding rate, in conditions of very short lasting (synaptic) GABA transients, is expected to reduce the percentage of fully bound receptors in response to synaptically released GABA. Thus, the combination of a reduction of agonist binding rate with a short lasting synaptic agonist transient is likely to produce a larger current inhibition than in the case of current responses to exogenous GABA application (for which agonist application lasts much longer than that in the synaptic cleft). It is noteworthy that a higher 'resistance' to inhibition by OETX of responses elicited by high GABA concentrations in comparison to those evoked by low agonist levels (compare Figures 4–6) is compatible with the view that at least a part of the toxin's effect is due to reduction of the agonist binding rate. It cannot be excluded, however, that a pronounced effect of OETX on mIPSCs might involve a presynaptic effect. Although a drop in mIPSC frequency in the presence of OETX (Figure 2) is consistent with strong amplitude reduction (making a proportion of mIPSCs not discernible against the baseline noise), we cannot exclude a presynaptic OETX action leading to a decrease in release probability and/or a change in quantal content.

Possible involvement of open channel block

The analysis of current responses to exogenous GABA suggests that OETX exerts an open channel block on $GABA_A$ receptors. This possibility is based on two observations: increased fading of current responses to 3 μM GABA (Figure 4C,D) and use dependence suggested by enhanced blockade of current evoked by a subsequent response to 10 mM GABA (Figure 6B,C). One could argue that OETX-induced enhancement of current fading for responses to 3 μM GABA could result from increased desensitization rate. This is, however, unlikely, because desensitization is strongly suppressed by OETX as demonstrated by the analysis of current responses to prolonged and saturating GABA concentrations (Figure 8A). On the other hand, increased fading of currents evoked by 3 μM GABA tended to disappear at higher OETX concentrations (Figure 4D). This observation, together with profound and complex OETX effects on the kinetics of current responses to exogenous GABA, clearly indicates that this toxin, in addition to a possible open channel block, strongly interferes with the binding and gating of $GABA_A$ receptors, and these effects become predominant at high OETX concentrations. It would be helpful to further verify the hypothesis of the open channel block by considering the effect of OETX on the single channel properties. However, excised patches in our cell cultures contained too many $GABA_A$ receptors to discern the single channel activity at the GABA concentrations we have used. At low GABA concentrations (up to 1 μM), interpretation of the single-channel data could be difficult because of substantial contribution from short-lived, singly bound events (Macdonald *et al*., 1989) and a disproportionate contribution from the high affinity δ subunit-containing receptors. It is interesting to note that the fading of responses to 3 μM GABA that suggests the

open channel block by OETX is characterized by a relatively slow kinetics, and therefore this mechanism would preferentially affect long-lasting tonic GABAergic inhibition (believed to be activated by ambient submicromollar GABA (Farrant and Nusser, 2005) rather than phasically active synaptic IPSCs.

As an alternative to the proposed mechanism of OETX-mediated $GABA_A$ receptor inhibition, a competitive antagonism could also be considered. Such a mechanism would predict, for instance, a slowing of current onset. However, the fact that OETX delays the onset of current response to saturating GABA concentrations by only approximately 10 ms suggests that interaction of OETX with GABA binding sites occurs within a millisecond time-scale. This proposal, however, is incompatible with observation that a 100 ms application of a saturating GABA concentration was not enough to complete the action of OETX (Figure 6B). Moreover, as mentioned in Results, the effect of OETX did not change when increasing GABA concentration from 10 to 30 mM, providing further evidence that competitive inhibition is not involved. In addition, the fact that in the presence of OETX the rising phase of currents evoked by short (1–3 ms) application of saturating GABA concentrations outlasts the duration of the GABA pulse (Figure 8B), cannot be explained by the competitive inhibition mechanism. The most consistent explanation for this observation is that OETX slows the conformational transitions between bound receptor states of $GABA_A$ receptors that underlie the current onset kinetics.

Biological impact of OETX and conclusions

The potent inhibition of GABAergic currents, known to play a crucial role in the inhibition in the adult CNS, would be an adequate explanation of the epileptogenic activity of OETX in the CNS (Chauvel *et al*., 1978; Louvel and Heinemann, 1980; 1983; Ball *et al*., 1987). However, OETX has been also demonstrated to block action potential generation and to interfere with Na^+ and K^+ channels (Dubois and Schneider, 1981; 1982). The relative contributions of GABAergic inhibition blockade and suppression of excitability to behavioural implications of intoxication with OETX remain to be elucidated.

Taken together, our results show that OETX potently inhibits both mIPSCs and currents elicited by exogenous GABA applications by a complex mechanism comprising allosteric modulation of binding and gating properties and a use-dependent blockade, compatible with the open channel block. The potent block of currents, including tonic currents, evoked by prolonged applications of low GABA concentrations by OETX may underlie, at least partially, induction of enhanced cell excitability which gives rise to the neurological symptoms of poisoning from water dropwort (*O. crocata* L.).

Acknowledgement

This work was supported by Wellcome Trust International Senior Research Fellowship in Biomedical Science (grant no. 070231/Z/03/Z).

Conflict of interest

I declare hereby that there is no conflict of interest.

References

Alexander SPH, Mathie A, Peters JA (2009). *Guide to Receptors and Channels (GRAC)*, 4th edn. *Br J Pharmacol* **158** (Suppl. 1): S1–S254.

Andjus PR, Stevic-Marinkovic Z, Cherubini E (1997). Immunoglobulins from motoneurone disease patients enhance glutamate release from rat hippocampal neurones in culture. *J Physiol* **504**: 103–112.

Anet EFLJ, Lythgoe B, Silk MH, Trippet S (1953). Oenanthotoxin and cicutoxin: isolation and structures. *J Chem Soc* **62**: 309–322.

Appendino G, Pollastro F, Verotta L, Ballero M, Romano A, Wyrembek P *et al.* (2009). Polyacetylenes from Sardinian *Oenanthe fistulosa*: a molecular clue to risus sardonicus. *J Nat Prod* **72**: 962–965.

Bai D, Zhu G, Pennefather P, Jackson MF, MacDonald JF, Orser BA (2001). Distinct functional and pharmacological properties of tonic and quantal inhibitory postsynaptic currents mediated by gamma-aminobutyric acid(A) receptors in hippocampal neurons. *Mol Pharmacol* **59**: 814–824.

Ball MJ, Flather ML, Forfar JC (1987). Hemlock water dropwort poisoning. *Postgrad Med J* **63**: 363–365.

Bruneton J (1999). *Toxic Plants Dangerous to Humans and Animals*. Lavoisier Publishing: Paris, pp. 105–107.

Chauvel P, Louvel J, Anger JP, Chauvel Y (1978). Convulsions induced by enanthotoxin in the rat: correlation between electrophysiological modifications and clinical signs. *C R Acad Sci Hebd Seances Acad Sci D* **286**: 1833–1836.

Clarks EG, Kidder DE, Robertson WD (1949). Toxic principle of *Oenanthe crocata*. *J Pharm Pharmacol* 377–381.

Clements JD (1996). Transmitter timecourse in the synaptic cleft: its role in central synaptic function. *Trends Neurosci* **19**: 163–171.

Clements JD, Lester RA, Tong G, Jahr CE, Westbrook GL (1992). The time course of glutamate in the synaptic cleft. *Science* **258**: 1498–1501.

Downs C, Phillips J, Ranger A, Farrell L (2002). A hemlock water dropwort curry: a case of multiple poisoning. *Emerg Med J* **19**: 472–473.

Dubois JM, Schneider MF (1981). Block of Na current and intramembrane charge movement in myelinated nerve fibres poisoned with a vegetable toxin. *Nature* **289**: 685–688.

Dubois JM, Schneider MF (1982). Block of ionic and gating currents in node of Ranvier with oenanthotoxin. *Toxicon* **20**: 49–55.

Farrant M, Nusser Z (2005). Variations on an inhibitory theme: phasic and tonic activation of GABA(A) receptors. *Nat Rev Neurosci* **6**: 215–229.

Jonas P (1995). Fast application of agonists to isolated membrane patches. In: Sakmann B, Neher E (eds). *Single-Channel Recording*. Plenum Press: New York/London, pp. 231–243.

Jones MV, Westbrook GL (1995). Desensitized states prolong GABAA channel responses to brief agonist pulses. *Neuron* **15**: 181–191.

Louvel J, Heinemann U (1980). Diminution of the extracellular concentration of calcium ions during focal epileptic crisis induced by enanthotoxin in the cat cortex. *C R Seances Acad Sci D* **291**: 997–1000.

Louvel J, Heinemann U (1983). Changes in $[Ca^{2+}]0$, $[K^+]0$ and neuronal activity during oenanthotoxin-induced epilepsy in cat sensorimotor cortex. *Electroencephalogr Clin Neurophysiol* **56**: 457–466.

Macdonald RL, Rogers CJ, Twyman RE (1989). Kinetic properties of the GABAA receptor main conductance state of mouse spinal cord neurones in culture. *J Physiol* **410**: 479–499.

Maconochie DJ, Zempel JM, Steinbach JH (1994). How quickly can GABAA receptors open? *Neuron* **12**: 61–71.

Mozrzymas JW (2004). Dynamism of GABA(A) receptor activation

shapes the 'personality' of inhibitory synapses. *Neuropharmacology* **47**: 945–960.

Mozrzymas JW, Barberis A, Michalak K, Cherubini E (1999). Chlorpromazine inhibits miniature GABAergic currents by reducing the binding and by increasing the unbinding rate of GABAA receptors. *J Neurosci* **19**: 2474–2488.

Mozrzymas JW, Barberis A, Mercik K, Zarnowska ED (2003a). Binding sites, singly bound states, and conformation coupling shape GABA-evoked currents. *J Neurophysiol* **89**: 871–883.

Mozrzymas JW, Zarnowska ED, Pytel M, Mercik K (2003b). Modulation of GABA(A) receptors by hydrogen ions reveals synaptic GABA transient and a crucial role of the desensitization process. *J Neurosci* **23**: 7981–7992.

Mozrzymas JW, Wojtowicz T, Piast M, Lebida K, Wyrembek P, Mercik K (2007). GABA transient sets the susceptibility of mIPSCs to modulation by benzodiazepine receptor agonists in rat hippocampal neurons. *J Physiol* **585**: 29–46.

Newland CF, Cull-Candy SG (1992). On the mechanism of action of picrotoxin on GABA receptor channels in dissociated sympathetic neurones of the rat. *J Physiol* **447**: 191–213.

Overstreet LS, Westbrook GL, Jones MV (2002). Measuring and modeling the spatiotemporal profile of GABA at the synapse. In: Quick M (ed.). *Transmembrane Transporters*. Wiley Interscience: New York, pp. 259–275.

Stell BM, Mody I (2002). Receptors with different affinities mediate phasic and tonic GABA(A) conductances in hippocampal neurons. *J Neurosci* **22**: RC223.

Teuscher E, Lindequist U (1994). *Biogene Gifte: Biologie, Chemie, Pharmakologie*. Fischer Verlag: Stuttgart, pp. 30–34.